Picozzi, M., Bindi, D., Spallarossa, D., Oth, A., Di Giacomo, D., Zollo, A. (2019): Moment and energy magnitudes: diversity of views on earthquake shaking potential and earthquake statistics. - *Geophysical Journal International*, *216*, 2, pp. 1245—1259.

DOI: http://doi.org/10.1093/gji/ggy488

Geophysical Journal International

Geophys. J. Int. (2019) **216,** 1245–1259
Advance Access publication 2018 November 21
GJI Seismology

doi: 10.1093/gji/ggy488

Moment and energy magnitudes: diversity of views on earthquake shaking potential and earthquake statistics

M. Picozzi,[1] D. Bindi,[2] D. Spallarossa,[3] A. Oth,[4] D. Di Giacomo[5] and A. Zollo[1]

[1] *Physics Department, University of Naples Federico II, Italy. E-mail: matteo.picozzi@unina.it*
[2] *Helmholtz Centre Potsdam, GFZ German Research Centre for Geosciences, Telegrafenberg, 14473 Potsdam, Germany*
[3] *DISTAV, University of Genova, Italy*
[4] *European Center for Geodynamics and Seismology, Walferdange, Luxembourg*
[5] *International Seismological Centre ISC, Thatcham, Berkshire, United Kingdom*

Accepted 2018 November 17. Received 2018 November 14; in original form 2018 June 12

SUMMARY

The size of an earthquake can be defined either from the seismic moment (M_0) or in terms of radiated seismic energy (E_r). These two parameters look at the source complexity from different perspectives: M_0 is a static measure of the earthquake size, whereas E_r is related to the rupture kinematics and dynamics. For practical applications and for dissemination purposes, the logarithms of M_0 and E_r are used to define the moment magnitude M_w and the energy magnitude M_E, respectively. The introduction of M_w and M_E partially obscure the complementarity of M_0 and E_r. The reason is due to the assumptions needed to define any magnitude scale. For example, in defining M_w, the apparent stress (i.e. the ratio between M_0 and E_r multiplied by the rigidity) was assumed to be constant, and under this condition, M_w and M_E values would only differ by an off-set which, in turn, depends on the average apparent stress of the analysed data set. In any case, when the apparent stress is variable and, for example, scales with M_0, the value of M_E derived from M_w cannot be used to infer E_r.

In this study, we investigate the similarities and differences between M_w and M_E in connection with the scaling of the source parameters using a data set of around 4700 earthquakes recorded at both global and regional scales and belonging to four data sets. These cover different geographical areas and extensions and are composed by either natural or induced earthquakes in the magnitude range $1.5 \leq M_w \leq 9.0$. Our results show that M_E is better than M_w in capturing the high-frequency ground shaking variability whenever the stress drop differs from the reference value adopted to define M_w. We show that M_E accounts for variations in the rupture processes, introducing systematic event-dependent deviations from the mean regional peak ground motion velocity scaling. Therefore, M_E might be a valid alternative to M_w for deriving ground motion prediction equations for seismic hazard studies in areas where strong systematic stress drop scaling with M_0 are found, such as observed for induced earthquakes in geothermal regions. Furthermore, we analyse the different data sets in terms of their cumulative frequency–magnitude distribution, considering both M_E and M_w. We show that the b values from M_w (b_{Mw}) and M_E (b_{ME}) can be significantly different when the stress drop shows a systematic scaling relationship with M_0. We found that b_{ME} is nearly constant for all data sets, while b_{Mw} shows an inverse linear scaling with apparent stress.

Key words: Earthquake dynamics; Earthquake ground motions; Earthquake source observations; Statistical seismology.

1 INTRODUCTION

The earthquake magnitude is one of the most fundamental earthquake source parameters for several reasons: seismologists quantify and convey the earthquake size to the public using this parameter; its rapid determination allows for a timely dissemination of the ground motion experienced in the area struck by an earthquake (i.e. shaking maps; Worden *et al.* 2010) and the implementation of emergency plans; and it represents one of the key parameters in the generation of seismic catalogues, which are the basis for processing large numbers of events and carrying out Probabilistic Seismic Hazard

Assessment (PSHA) studies, just to mention some of its most common uses. Despite its importance, it is largely recognized that it is not possible to characterize the full extent of earthquake source complexity (e.g. fault length and area; velocity, acceleration and duration of fault motion; amount of radiated energy; and a combination of these; Kanamori 1983) through the use of one single source parameter.

Since the introduction of the local earthquake magnitude scale M_L by Richter (1935), different scales have been proposed to accommodate different purposes. Whilst most of the magnitude scales are empirical (i.e. determined by measuring a seismic wave amplitude at a given period and correcting for the amplitude attenuation with distance), the moment magnitude M_w and the energy magnitude M_E are the only two physical (and not-saturating) magnitude scales. These are indeed defined from two seismic source parameters: the seismic moment (M_0, Aki 1968; Kanamori & Anderson 1975) for M_w, and the seismic energy (E_r) radiated by the source through seismic waves (Gutenberg 1945b; Gutenberg & Richter 1956; Aki 1968; Hanks & Kanamori 1979) for M_E. These two source parameters look at the source complexity from different perspectives: M_0 is a static measure of the earthquake size, whereas E_r is connected to the rupture kinematics and dynamics (e.g. Bormann & Di Giacomo 2011a).

A well-established methodology exists for the determination of M_w, which is routinely used in seismic observatories and is generally considered as the primary measure of the earthquake size by the seismological community. It is important to stress that M_w, being based on an estimate of the seismic moment M_0, which in turn represents the long-period end of the source spectrum and is proportional to the fault area and to the average slip, it provides a tectonic measure of the earthquake size. Considering the self-similarity of the source spectra (Aki 1967), only in the case of a constant stress drop independent of magnitude, a single source parameter would be sufficient to describe the scaling of the source spectrum with the earthquake size. Evidence for the contrary is rather overwhelming. For instance, earthquakes with the same M_w can give rise to larger ground motions with the increase of the stress drop $\Delta\sigma$ (Baltay *et al.* 2013), the latter controlling the amount of energy radiated by the source at high frequencies for a given M_0 (e.g. Anderson 1997). Therefore, the observed variability of stress drop over several orders of magnitudes (e.g. Courboulex *et al.* 2016, and references therein) suggests that M_0 and E_r are both needed to fully characterize the earthquake size and its strength. E_r, being related to the rupture velocity and stress drop, provides a measure of the earthquake strength and its potential of causing shaking damage (hereinafter, earthquake shaking potential; Bormann 2015). In our opinion, the introduction of M_w and M_E partially obscured the complementarity of M_0 and E_r, and the reason lies in the assumptions needed to define any magnitude scale. For example, in defining M_w, the apparent stress, τ_a, (i.e. $\tau_a = \mu\ E_R/M_0$, where μ is the rigidity) was assumed constant (Kanamori 1977). Under this condition, M_w and M_E values would only differ by an off-set which, in turn, depends on the average apparent stress of the analysed data set (Bormann & Di Giacomo 2011a). In any case, whenever the apparent stress is variable and, for example, depends on M_0, the value of M_E derived from M_w cannot be used to infer E_r.

M_w plays a significant role in Probabilistic Seismic Hazard Assessment (PSHA) analyses, a context where it is a key predictive variable for modelling the source-related contributions to ground shaking. Indeed, Ground Motion Prediction Equations (GMPEs) calibrated on M_w are typically used to compute both the median predictions and the aleatory variability for any seismic scenario of interest (e.g. Douglas & Edwards 2016). In recent years, significant efforts have been made to find other source-related explanatory variables (e.g. style of faulting) to complement M_w, with the purpose of decreasing the event-specific component of the aleatory variability (also called between-event or inter-event variability, Al-Atik *et al.* 2010), which absorbs repeated source effects not captured by magnitude differences among the analysed earthquakes. $\Delta\sigma$ and its variability among earthquakes has been the object of several recent studies (e.g. Anderson & Lei 1994; Bindi *et al.* 2006, 2017; Baltay *et al.* 2017; Oth *et al.* 2017) and has been found to correlate well with the between-event residuals at short periods. These studies provide hints that rapid estimates of $\Delta\sigma$ may allow for more reliable predictions of the earthquake shaking. However, measurement errors on $\Delta\sigma$ are generally very large, and the difficulties in its estimation for past earthquakes can represent a limit to its widespread use.

In the framework of the discussion within the hazard community on the combined use of M_w with other source parameters for the refinement of the variability models (Douglas & Edwards 2016), this work aims at bringing the attention on the energy magnitude M_E as alternative scale to M_w in seismic hazard applications, as inspired by the common roots and differences of M_w and M_E discussed by Bormann & Di Giacomo (2011a) and Bormann (2015), and the study of Atkinson (1995) on the optimal choice of magnitude scales for seismic hazard assessment.

The aim of this study is to investigate similarities and differences between M_w and M_E in relation to the scaling of source parameters over a broad magnitude range. As outlined in the following sections, in this work we refer to the M_E defined according to the 'Gutenberg–Richter' relationship (Richter 1958). The assessment of the impact of the assumptions behind the definition of M_w when the self-similarity of the source scaling is violated is of particular interest for this study. To accomplish such a goal, we use four different data sets whose source parameters (i.e. seismic moment, M_0, corner frequency, f_c, or directly the seismic radiated energy, E_r) are available from previous studies: a global data set including earthquakes with $M_w > 5.5$ (Di Giacomo *et al.* 2010); a regional data set including earthquakes in the magnitude range 2.7–7.2 that occurred in Japan (Oth 2013); a local data set including earthquakes in the magnitude range 2.5–6.5 that occurred in Central Italy (Bindi *et al.* 2018); and finally, a data set for induced events within The Geyser geothermal area (Picozzi *et al.* 2017a) in the magnitude range 1.5–4.

Regarding the use of these data sets, we note that we did not merge or combine the data sets during our processing. With the only exception of the section where we discuss the scaling of M_w and M_E in relation to the stress drop ($\Delta\sigma$), we always consider each data set separately, as stressed by the usage of different colours for different data sets. The joint discussion of the data sets pertains to the outcomes from different studies performed by the same authors using almost identical methodologies (except for the global data set).

In the following, after providing a summary of the assumptions behind the relations to compute M_w and M_E, we discuss the application of the two magnitude scales to the four data sets from two different points of view: capturing the event-to-event variability of the peak ground velocity and their implications on the characteristics of the cumulative frequency–magnitude (CFM) distributions.

2 METHOD AND DATA SETS

In this study, the regional and local M_0 and E_r estimates have been obtained applying the Generalized Inversion Technique (GIT; e.g.

among others, Castro *et al.* 1990; Oth *et al.* 2011). The GIT approach used in all these cases is a non-parametric and data-driven inversion scheme capable of extracting from *S*-wave Fourier Amplitude Spectra empirical functions of the source, site and attenuation. One of the main advantages of this GIT method consists in performing the inversion in a non-parametric way, that is, without imposing any a priori assumption on the functional form of the attenuation operator. This feature allows us to avoid assumptions on Q or geometrical spreading, but still capture attenuation trends related to distance as well as the effect of later arrivals. In particular, E_r was derived from the GIT's M_0 and corner frequency (f_c) estimates following Izutani & Kanamori (2001):

$$E_r = \frac{4\pi}{5\rho v_S^5} \int_0^\infty |fM(f)|^2 df, \quad (1)$$

where $M(f)$ represents the source model in displacement, v_S and ρ are the *S*-wave velocity and density in the source region, respectively. In the cases of the Italian and The Geysers data sets, $M(f)$ is represented by a theoretical source model derived considering the obtained estimates of M_0 and f_c (i.e. $M(f) = \frac{M_0}{1+(\frac{f}{f_c})^\gamma}$; whereas the parameter γ controlling the high-frequency spectral fall-off is equal to 2 for the Italian data, corresponding to the Brune's source model (Brune 1970) and variable between 2 and 3 for The Geysers, Picozzi *et al.* 2017a). In the case of the Japanese data set, $M(f)$ was obtained by the frequency band-limited empirical source spectra derived from GIT combined with the Brune's source model (Brune 1970) at frequencies lower and higher than those limiting the empirical one. This extrapolation was carried out to account for the missing energy outside the frequency band of the empirical source spectra as highlighted by Ide & Beroza (2001). Fig. S1 shows that the two approaches for computing E_r provide consistent results for the Japanese data set. Similarly, also comparing E_r relevant to different regions and source spectra integration strategies (i.e. the Italian and Japanese data sets) the results are very similar for the largest magnitude earthquakes and show the same E_r-to-M_0 scaling (Fig. S2). The use of eq. (1) for computing E_r applying one of the two source spectra integration strategies has, during the years, become a *de facto* standard (e.g. among the others, Venkataraman *et al.* 2002; Venkataraman & Kanamori 2004; Oth 2013).

2.1 Worldwide earthquakes

This data set consists of 712 worldwide shallow earthquakes (i.e. depth < 70 km) in the magnitude range $5.5 \leq M_w \leq 9.0$ (Fig. 1a). The considered earthquakes occurred between 1990 and 2007, plus the M_w 7.9 Wenchuan earthquake of 2008 (Di Giacomo *et al.* 2010). The data set is strongly dominated by thrust and strike-slip earthquakes. We rely on teleseismic E_r and M_E estimates derived by Di Giacomo & Bormann (2011), where the analysis was carried out on the vertical component of broad-band recordings from both global and regional networks. The M_0 and M_w estimates were obtained from the Global Centroid Moment Tensor (GCMT, www.globalcmt.org, Dziewonski *et al.* 1981; Ekstrom *et al.* 2012) database.

2.2 Japan

The data set consists of 1949 shallow earthquakes (i.e. depths smaller than 30 km) that occurred in the Japanese area in the period from 1996 to 2011 and in M_w range from 2.7 to 7.2 (Fig. 1b). The recordings are from the KiK-net and K-NET accelerometric networks (Okada *et al.* 2004). Although the data set is populated by various styles of faulting, the prevalent types are thrust and strike-slip. Source parameters (i.e. M_0, $\Delta\sigma$ and corner frequency f_c) have been derived by Oth (2013) from a one-step non-parametric generalized inversion technique (GIT). As discussed above, E_r estimates were obtained by eq. (1).

2.3 Central Italy

The data set includes 1365 earthquakes in the M_w range from 2.5 to 6.5 recorded during the main seismic sequences over the past 10 yr in Central Italy: the 2009 L'Aquila sequence, and the 2016–2017 Central Italy sequence (Fig. 1c). The data include both velocimetric and accelerometric recordings provided by both permanent and temporary networks: The National Seismic Network (RSN), the Mediterranean Network (Mednet), the Rapid Response Networks operated by the Istituto Nazionale di Geofisica e Vulcanologia (INGV), and the National Accelerometric Network (RAN) operated by the Department of Civil Protection (DPC). Over 75 per cent of depths are shallower than 10 km. The central Apennine belt in Italy is characterized since Middle Pliocene by southwest–northeast extension (Pace *et al.* 2006). Therefore, most earthquakes analysed by Bindi *et al.* (2018) are associated with pure normal faulting. Source parameters (i.e. corner frequency f_c, seismic moment M_0, and stress drop $\Delta\sigma$) were estimated by Bindi *et al.* (2018) using a GIT approach, whereas E_r estimates were obtained by exploiting M_0, f_c in eq. (1).

2.4 The Geysers (TG)

Located in California and in operation since the 1960s, TG is the largest vapour-dominated geothermal reservoir in the world. The most interesting feature of this data set is that the 633 earthquakes analysed are all induced and located at depth shallower than 4 km (i.e. within the geothermal reservoir), where temperatures are high (varying between ~240 and ~340 °C). Magnitudes are in the M_w range 1.5–4, and with dominance of strike-slip and normal faulting mechanisms. These events have occurred between 2009 and 2011 and were recorded by 32 three-component stations of the Lawrence Berkeley National Laboratory Geysers/Calpine (BG) surface seismic network. The seismic stations are distributed over a 20 km by 10 km area which covers the entire geothermal field (Fig. 1d). Recordings are freely available via the Northern California Earthquake Data Center (NCEDC). As for the Central Italy data set, source parameters (M_0, $\Delta\sigma$ and f_c) are obtained by applying a GIT approach (Picozzi *et al.* 2017a) and the Izutani & Kanamori (2001) approach to obtain E_r. It is worth noting that obtaining robust E_r estimates for small magnitude earthquakes, as those of the TG data set, is still a topic of current research. Just recently, Bindi *et al.* (2018) investigated the possibility of estimating E_r at regional scale in Italy and obtained robust E_r estimates for a range of magnitudes between M_w 2 and M_w 6.5. Furthermore, the theoretical study on the reliability of estimates of source parameters of small earthquakes recently presented by Kwiatek & Ben-Zion (2016) indicates that, considering the sensor characteristics, the hypocentral distances, the magnitude range and the level of seismic noise in the TG data, reliable earthquake source parameters (i.e. M_0 and f_c), and hence also E_r, can be estimated for the range of magnitude analysed by Picozzi *et al.* (2017a).

It is worth noting that for data sets (b), (c) and (d), the M_0 and E_r estimates stem from source spectra obtained by the GIT approach,

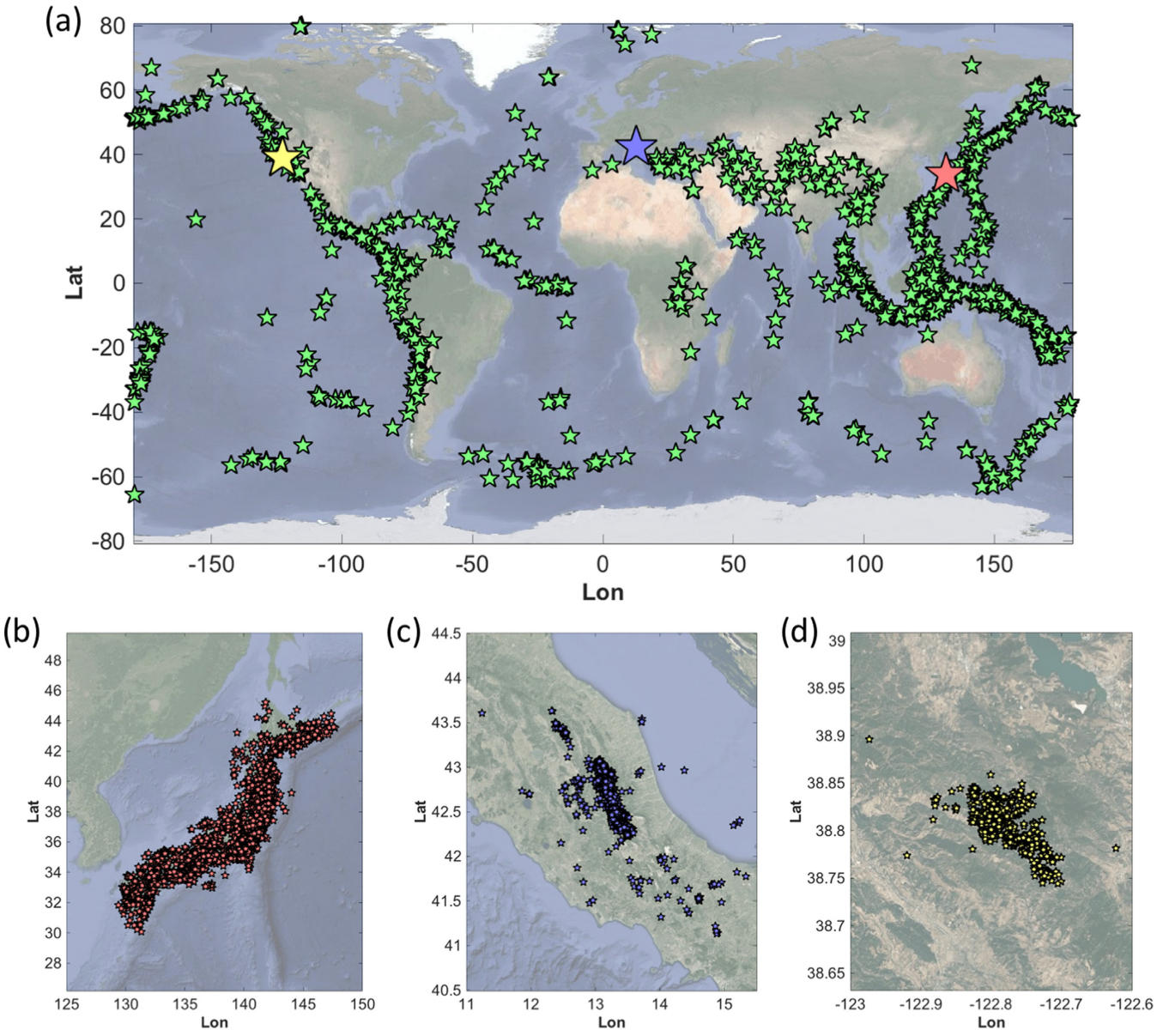

Figure 1. Locations of the earthquakes considered in this study for different data sets: (a) global teleseismic events (green), Japanese ones (red), Italian ones (blue) and The Geysers (TG) ones (yellow). (b) zoom in of the epicentral area of Japan. (c) as (b), but for Italy. (d) as (b), but for TG.

which allows for a robust quantification of systematic differences in using M_w or M_E as metric for quantifying the earthquake shaking potential or characterizing the cumulative frequency–magnitude (CFM) distributions.

3 MOMENT AND ENERGY MAGNITUDE

Besides the original papers, an exhaustive discussion on the origin of M_w and M_E is presented in Bormann & Di Giacomo (2011a, b). For the sake of clarity, we summarize the main concepts and assumptions of both magnitude scales in the following discussion.

Kanamori (1977) and Hanks & Kanamori (1979) derived the moment magnitude M_w starting from the Gutenberg–Richter relation between E_r and the surface magnitude M_S (Gutenberg 1945a), assuming a given dynamic fracture model (i.e. the 'Orowan model'; Orowan 1960).

The moment magnitude M_w is thus defined as:

$$M_w = (\log M_0 - 9.1)/1.5 = (\log M_0 - 4.3 - 4.8)/1.5, \quad (2)$$

where the slope value of 1.5 and the constant –4.8 are inherited from the M_S and $\log(E_r)$ relationship. The term –4.3 would correspond to $\log(E_r/M_0)$ (i.e. the slowness parameter Θ, Newman & Okal 1998), but it became a constant under the following assumptions made by Kanamori (1977) for 'very large earthquakes': (i) the energy required for fracturing is negligible; (ii) the final average stress and the average stress during faulting are equal (also known as 'complete stress drop' $\Delta\sigma$ or 'Orowan's model'); (iii) under average crust-upper mantle conditions, the average rigidity in the source area (μ) ranges from 3 to 6 $\times$ 10^4 MPa and (iv) for very large earthquakes $\Delta\sigma$ is nearly constant in the range between 2 and 6 MPa.

As highlighted by Bormann & Di Giacomo (2011b), during the past 40 yr, M_w has been applied by users over a wide range of magnitude (e.g. among many others, down to magnitude –1.8 by Oye

et al. 2005, down to –4.4 by Kwiatek *et al.* 2010, and down to –2.7 by Boettcher *et al.* 2015; in these studies, induced seismicity in mines was considered) without entering into the validity of the underlying assumptions that led Kanamori (1977) to constrain $\log(E_r/M_0) = -4.3$ (hereinafter, Θ_K).

Fig. 2(a) shows the M_0-to-E_r scaling for the four data sets with respect to the Kanamori condition of $\Theta_K = -4.3$. Interestingly, for most moderate to great magnitude earthquakes (i.e. $M_0 > 10^{16}$ N·m), Kanamori's scaling is reasonably well followed, even though for many of them, an almost constant shift downward is observed. On the contrary, smaller magnitude events (i.e. $M_0 < 10^{16}$ Nm) show a progressive, significant deviation downwards, leading to a much smaller radiated energy per seismic moment unit than that expected by Kanamori's assumptions.

Fig. 2(b) shows the distribution of empirical Θ values with respect to Θ_K. In principle (Figs 2a and b) show the same result, but from the latter point of view, the deviation of a great part of the earthquakes from Θ_K is much more evident. Fig. 2(b) suggests that most of the considered earthquakes can potentially generate a ground shaking variability at high frequency larger than the variability expected by assuming constant Θ as in eq. (2).

Following Purcaru & Berckhemer (1978), and having for each event independent M_0 and E_r estimates, we have been enticed to modify eq. (2) by including the individual event $\Theta = \log(E_r/M_0)$ instead of $\Theta_K = -4.3$, as follows:

$$\begin{aligned} M &= (\log M_0 + \Theta - 4.8)/1.5 \\ &= (\log M_0 + \log(E_r/M_0) - 4.8)/1.5, \end{aligned} \quad (3)$$

which leads to define an energy magnitude scale:

$$M_E = (\log E_r - 4.8)/1.5. \quad (4)$$

Eq. (4) correspond to the 'Gutenberg–Richter' energy–magnitude relationship (Richter 1958; Kanamori 1977; Choy & Boatwright 1995).

It is worth noting, that eq. (4) does not correspond to the M_E definition adopted by Choy & Boatwright (1995) [i.e. energy magnitude $M_e = (\log E_r - 4.4)/1.5$], not even to the strain-energy magnitude proposed by Purcaru & Berckhemer (1978). As explained by Bormann (2015), the origin for the different constant term 4.4 instead of 4.8 is due to the result of a fit between $\log(E_r)$ with M_S (~400 earthquakes with magnitude ≥ 5.8 occurred between 1986 and 1991, and reconfirmed with 2317 earthquakes from 1986 to 2012 by Choy 2012) and constraining the slope to 1.5 to guarantee a continuity with Richter's energy–magnitude definition (Richter 1958). However, sharing the rational basis of 'Gutenberg–Richter' energy—magnitude definition [i.e. the logic progress from eq. (2) to eq. (4)], in this study we prefer to adopt eq. (4) to derive M_E.

Fig. 2(a) shows that M_w and M_E agree well for $M_w > 5$, while for smaller magnitude events M_w tends progressively to be larger than M_E. The availability of $\Delta\sigma$ estimates, except for the data set of worldwide distributed events, allows us to highlight how the differences between M_w and M_E are related to $\Delta\sigma$. (Figs 3a and b) show that the (M_E–M_w) difference increases with decreasing $\Delta\sigma$. The $\Delta\sigma$ variability introduces a spread in the seismic energy versus moment distribution, which in terms of magnitude determines a difference of up two M_E units for earthquakes with the same M_w. Keeping in mind these differences between M_w and M_E in relation to $\Delta\sigma$, in the next section we explore the impact of using M_w and M_E as information to assess the earthquake shaking potential and in terms of Gutenberg–Richter law.

4 PEAK GROUND VELOCITY VARIABILITY USING M_w AND M_E

Although it is a widespread practice within the seismological community to discuss the effects of different dynamic seismic source properties in terms of peak ground acceleration (PGA) (e.g. Trugman & Shearer 2018), peak ground velocity (PGV) has proven to provide a significantly better correlation with seismic demand (Bradley 2012), mainly because PGV is controlled by the seismic energy at intermediate frequencies. There are many examples in engineering seismology and earthquake engineering using PGV as a parameter for estimating macroseismic intensity and structural damage (e.g. Bommer & Alarcon 2006). For these reasons, we compute the between-event residuals (δBe; Al-Atik *et al.* 2010) for PGV to illustrate the benefits of using M_w and M_E. Since the shaking potential assessment is the focus of this analysis, we only consider the data sets collected at regional/local scale (i.e. the Japan, Italy and TG), for which a consistent number of recordings within a few hundreds of kilometres are available. Furthermore, to facilitate the comparison of results from different data sets, and considering that we are interested in a magnitude range which extends below the minimum magnitude usually considered in ground motion prediction equation (GMPE) analysis (i.e. $M_w < 4$), we performed for each data set a linear regression analysis to model the PGV scaling with distance and magnitude by searching the best-fitting parameters of the following equation:

$$\begin{aligned} \log(PGV) = A + B_1(M - M_{ref}) \\ + B_2(M - M_{ref})^2 + C\log(R), \end{aligned} \quad (5)$$

where M is on a case-by-case basis M_w and M_E, R is the hypocentral distance in km and PGV is in cm s^{-1}, and the reference magnitude M_{ref} is set equal to 3.5 for the Japan and Italy data sets, while equal to 1.5 for TG (i.e. the last well sampled magnitude within each data set). Similar to Oth *et al.* (2017), also in our case the ground motion model of eq. (5) is kept deliberately simple, since we do not have the ambition to set up a GMPE for hazard calculation. The aim of this work is to help clarify the role of different event size metrics in the modelling of the between-event variability of ground motion. The calibration is repeated twice, considering either M_w or M_E, and the results of the regression analyses are provided in (Table 1). Then, the between-event residuals (δBe) are computed as the average difference, for any given event, between the PGV measured at different stations and the corresponding values predicted by the GMPE. (Fig. 4) shows δBe for the different data sets and the different magnitude.

It is clear from (Fig. 4) that for all three data sets the standard deviation of δBe is generally reduced when M_w is replaced with M_E (i.e. linearly with the M_w–M_E differences, it decreases of the 4 per cent for the Japan data set; of 44 per cent for the Italian one; of the 65 per cent for TG). These results indicate that M_E better accounts for those variations in the rupture process that can introduce systematic event-dependent deviations from the mean regional PGV scaling. Similar results for Italy were found by Bindi *et al.* (2018), and for an earthquake early warning energy magnitude (i.e. derived on P-waves recorded at local scale) by Picozzi *et al.* (2017b). The comparison among (Figs 2 and 4) highlights that the reduced δBe variability is mostly related to earthquakes (i.e. generally with $M_w < 5$) for which the deviation from the Kanamori's condition $\Theta = \Theta_K$ is larger.

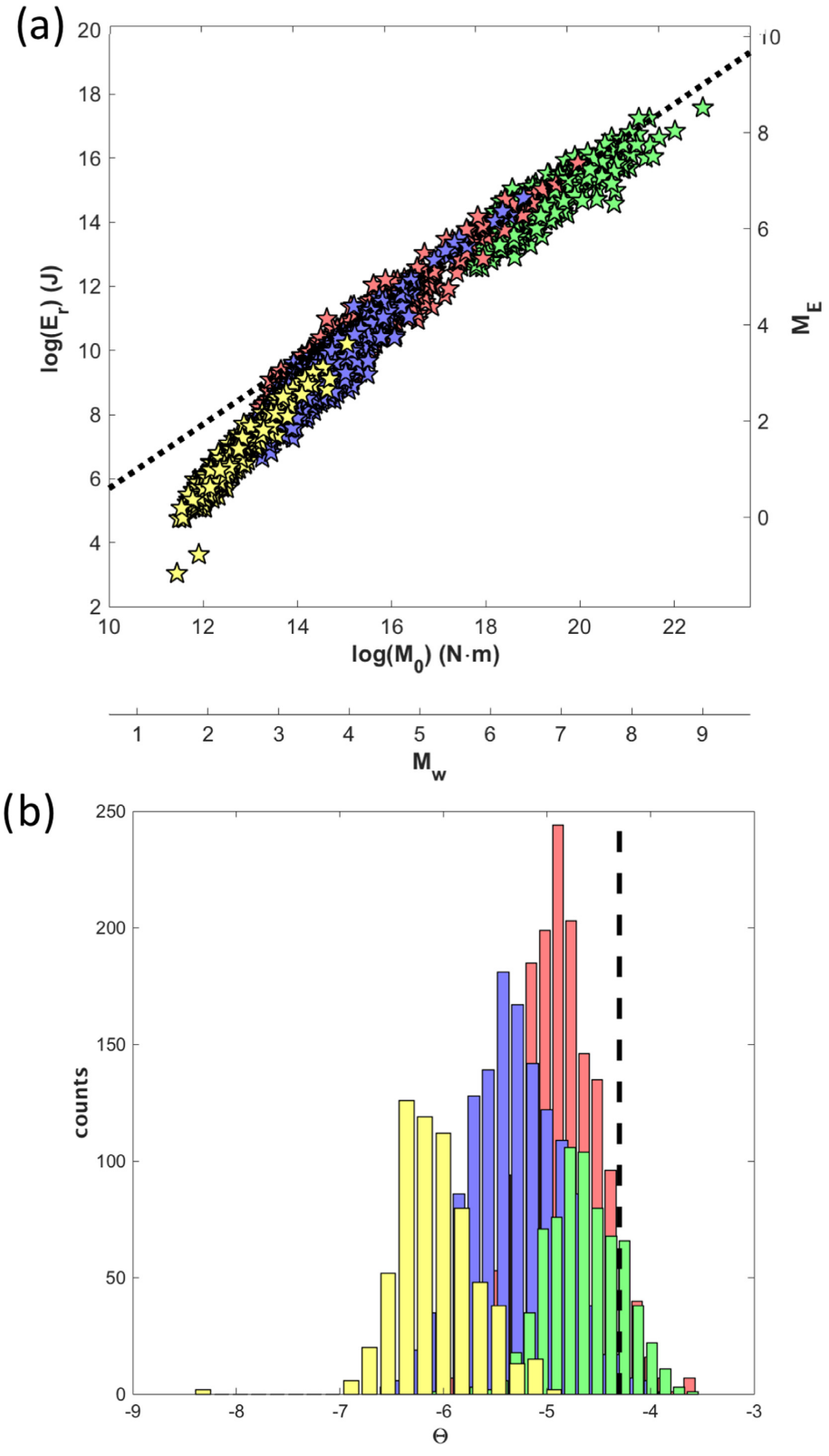

Figure 2. (a) E_r-to-M_0 scaling for the four data sets (data sets coloured accordingly to Fig. 1); additional axes are added for Moment magnitude (M_w) and energy magnitude (M_E). Scaling from Kanamori's assumption (dashed line). (b) Distribution of the slowness parameter, Θ, (i.e. same colour as before), and Θ corresponding to Kanamori's assumption (i.e. Θ_K, dashed line).

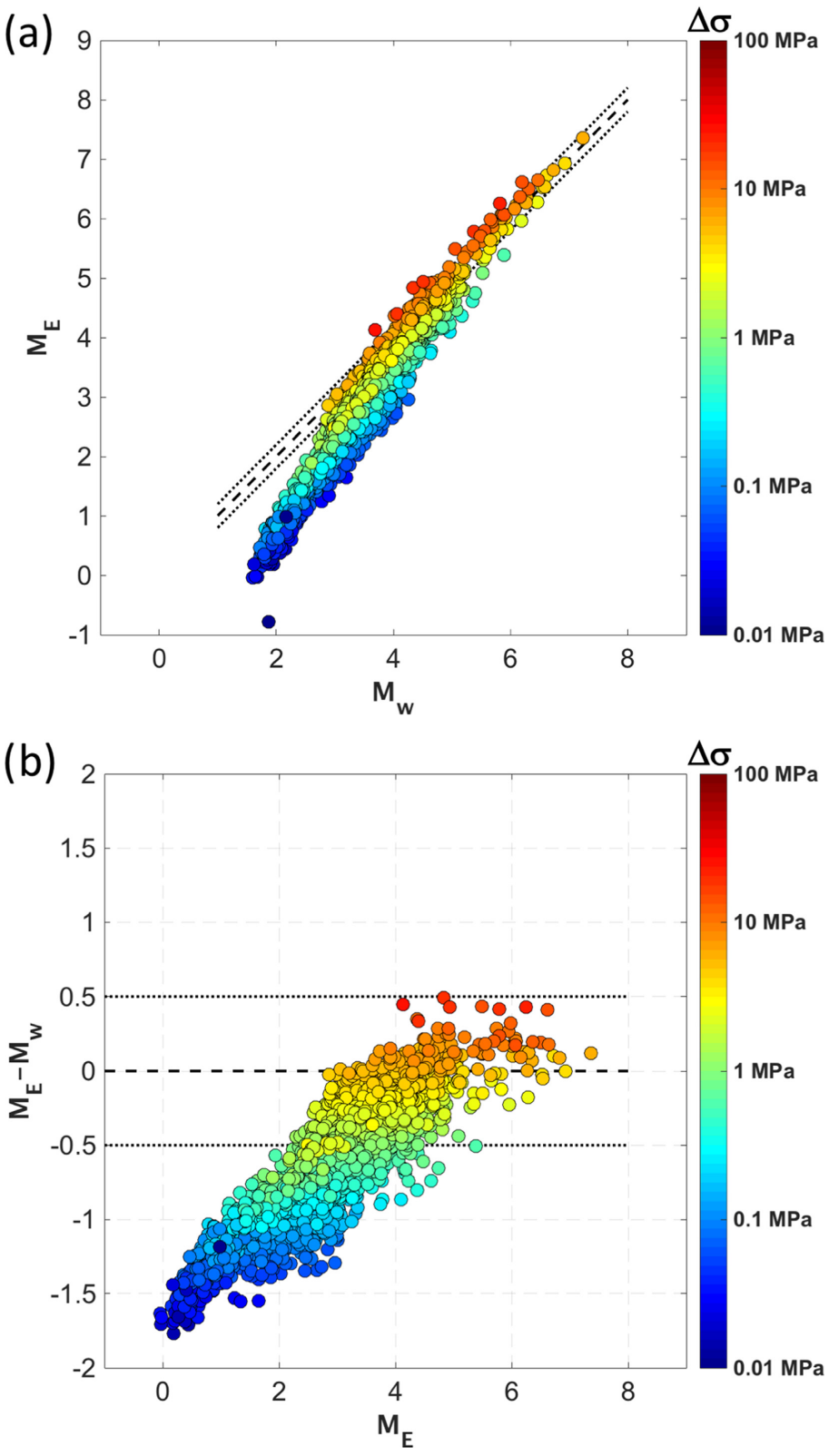

Figure 3. (a) M_w versus M_E for the Japanese, Italian and TG data sets, coloured per stress-drop, $\Delta\sigma$. (b) ($M_E - M_w$) differences versus M_E coloured per $\Delta\sigma$.

Table 1. Regression parameters of eq. (5) for different data sets and magnitude.

	A	B_1	B_2	C	Stand. dev.
M_w – Japan	0.83	0.72	0.02	–1.30	0.441
M_e – Japan	1.11	0.62	0.03	–1.34	0.424
M_w – Italy	0.75	1.08	–0.03	–1.64	0.230
M_e – Italy	1.36	0.78	–0.012	–1.69	0.139
M_w – TG	–2.46	1.38	–0.12	–2.07	0.144
M_e – TG	–1.16	0.73	–0.04	–2.07	0.069

5 CUMULATIVE FREQUENCY–MAGNITUDE DISTRIBUTION FOR M_w AND M_E

Similarly to Uchide & Imanishi (2018), we aim at highlighting how a different event size metric (i.e. M_w versus M_E), related to different physical parameters (i.e. M_0 or E_r), can affect earthquake statistical outcomes. However, it is worth noting that the data sets considered in this study were generated with the purpose of performing source parameter studies, and thus have been guided each by a different level of event selection with the aim of considering only high quality events/recordings among all those available within the authoritative database of origin. For instance, while the event selection was negligible for the Japanese, Italian and TG data sets, it was important in the case of the global one; thus, we decided to exclude this latter from the following statistical analysis. Even considering the incomplete nature of our data sets, for the sake of simplicity and of using a standard terminology within the seismological community, we will study in the following the CFM distributions adopting standard approaches used in seismic hazard.

Fig. 5 shows the comparison of CFM obtained for M_w and M_E, where for the sake of a simple comparison, we divided the data sets in different plots. Interestingly, whilst for the Japanese data set the two CFMs are very similar (Fig. 5a), we observe that they differ substantially for the Italian and TG data sets (Figs 5c and e, respectively).

The classic approach in earthquake statistics is studying the earthquake size distribution in terms of the Gutenberg–Richter law (Gutenberg & Richter 1942). Therefore, we parametrized the obtained CFM by the power law model known as Gutenberg–Richter law (*GR-law*), which is expressed as

$$\log N = a - bM, \tag{6}$$

where N is the cumulative number of earthquakes, a and b are parameters describing the productivity and relative event size distribution, respectively, and we will use the concept of completeness magnitude (Mc). As previously discussed, our aim is to compare the effects of using M_w and M_E on earthquake statistical outcomes, and we expressly warn the readers that our parameters (i.e. a, b and M_c) cannot be used for hazard calculation.

Eq. (6) was parametrized for the three data sets considering either M_w or M_E by exploiting the entire-magnitude-range method proposed by Woessner & Wiemer (2005). The latter is implemented in the software package ZMAP (Wiemer 2001) and allows for the simultaneous estimate of M_c, a and b (i.e. this latter obtained by the maximum likelihood approach proposed originally by Aki 1965 and Utsu 1965). The uncertainty of the parameters obtained is computed by means of a bootstrap approach (Efron 1979). For each data set 10 000 realizations of random sampling with replacement were performed.

The results are summarized in (Table 2) and (Fig. 5). The CFM distributions for TG data, where the stress drop scaling with seismic moment is the strongest, presents interesting features. Indeed, we observe that M_c decreases from 2.1 for M_w to 0.8 for M_E, while b drops from 1.15 (i.e. a value compatible with the range of b values obtained by Convertito *et al.* 2012 during a time-dependent PSHA study) to 0.68 for M_w and M_E, respectively (i.e. hereinafter indicated as b_{Mw} and b_{ME}). However, the CFM for M_E seems could be better described by an upper-truncated power law than by a power law. The origin of breaks in CFM is a topic of great interest for the scientific community and has been also explained as being due to the finite width of the seismogenic lithosphere (e.g. Pacheco *et al.* 1992; Scholz 1997; Main 2000; Burroughs & Tebbens 2002). This might be the case of the TG area, where the geothermal reservoir, which hosts the whole seismicity, is bounded at about 4 km of depth by Pleistocene felsite intrusion (Picozzi *et al.* 2017a). On the other hand, we highlight that the scaling of $\Delta\sigma$ with M_0 would imply that in the case of M_w the characterization of the seismicity CFM using a power-law functional form may be questionable. While we are aware that this is a far-reaching statement, the detailed analysis of this issue is beyond the scope of this paper and will be investigated in detail in future studies.

However, in order to quantify the variations observed in the traditional framework that most readers will be familiar with, in the following, we nevertheless examine a GR-fit to the CFM distributions, as discussed later.

Focusing on b-values, it is also relevant to note that the b-values for M_w ranges for the three data sets between 1.15 (i.e. TG) and 0.76 (i.e. for Japan), while in the case of M_E, the b-values span a narrower range (i.e. between 0.69 for the Italian data set and 0.65 for the Japanese, Table 2), as shown in (Fig. 6a) where b for M_w and M_E are represented with respect to both Θ and the apparent stress (i.e. $\tau_a = \mu\, E_r/M_0$, computed assuming a crustal shear modulus μ equal to 3.3×10^4 MPa). Concerning Θ, with high variability within each data set, we consider in (Figs 6a and d) the median $\pm$ the standard deviation of its distribution as a representative value for the whole data set. The different behaviour of b_{Mw} and b_{ME} stems from the different dynamic conditions under which earthquakes occur in the regions under study, an issue that can be mapped by studying how Θ is distributed with respect to M_0 and E_r. (Figs 6b and c) show that all data sets show a similar linear scaling of Θ with E_r (i.e. the b_{ME} are similar), but different with respect to M_0 (i.e. the b_{Mw} are different). For instance, these observations agree with the non-self-similar behaviour found by Picozzi *et al.* (2017a) for TG data set, and the overall close to self-similar scaling found for the Japanese data by (Oth *et al.* 2010; Oth 2013).

Considering the fact that b_{Mw} reflects the moment release, whilst b_{ME} reflects the energy release, we show in (Fig. 6d) that their difference (i.e. $b_{Mw} - b_{ME}$) is linearly correlated with the deviation from Kanamori's condition (i.e. measured as $\Theta - \Theta_K$). In particular, (Fig. 6d) shows that with an increase in the $(\Theta - \Theta_K)$ difference (i.e. which corresponds to a reduced amount of energy radiated per seismic moment unit than the one corresponding to the Kanamori's assumptions), also the $(b_{Mw} - b_{ME})$ difference increases.

6 DISCUSSION

We investigated similarities and differences between M_w and M_E in connection with the scaling of the source parameters over a broad magnitude range. Our results from the global, the Japanese and Italian data sets all agree in showing that for moderate to strong earthquakes (i.e. $M_w > 5$), Kanamori's condition (i.e. $\Theta \cong \Theta_K = -4.3$) is fulfilled, the E_r-to-M_0 scaling is almost constant, and thus

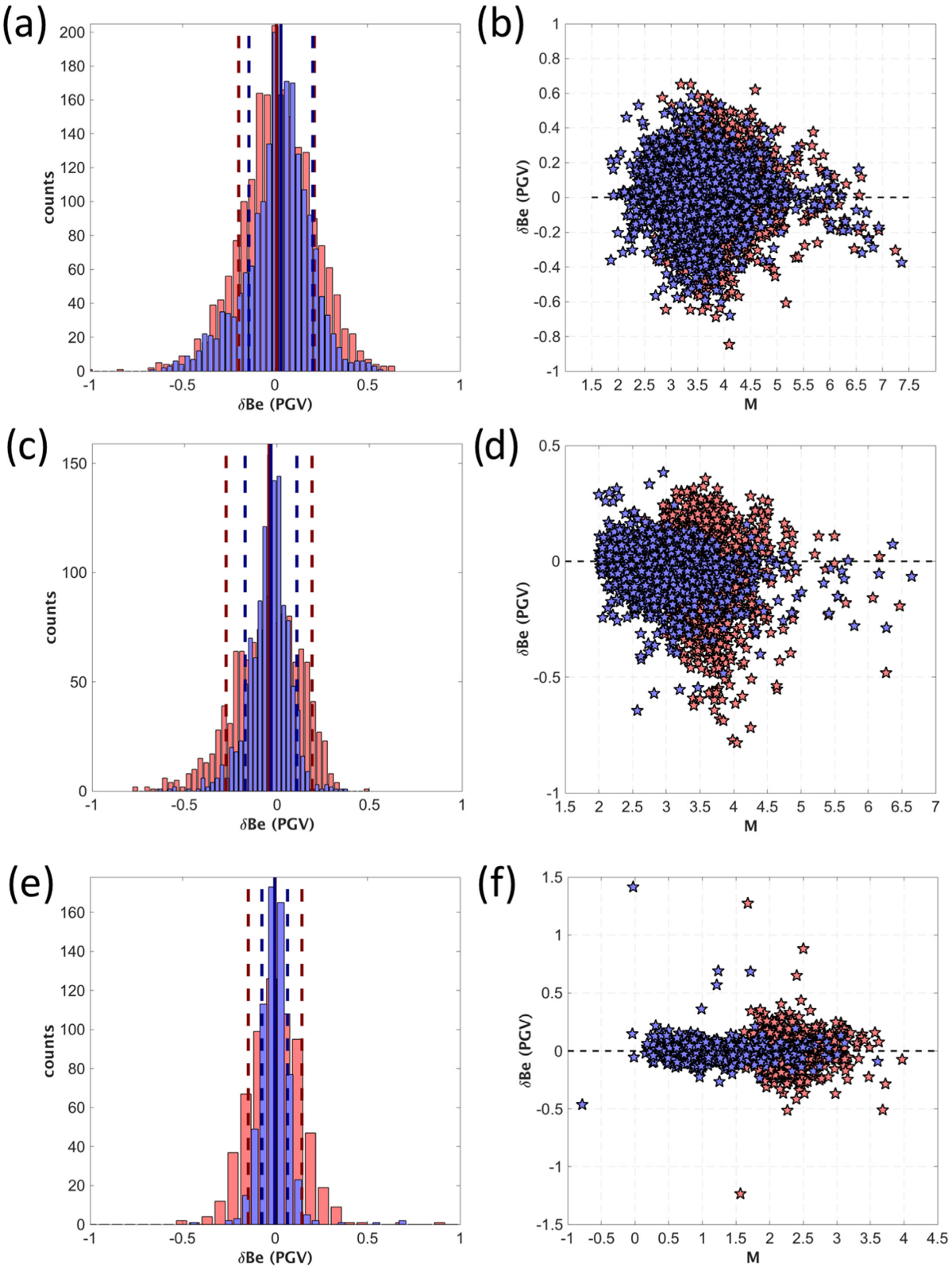

Figure 4. (a) Histograms of the between-event residuals (δBe) computed for PGV considering M_w (red) and M_E (blue) for the Japan data set; the ± 1 standard deviations are red and blue dashed lines for M_w and M_E, respectively. (b) δBe residuals for PGV considering either M_w (red) or M_E (blue) versus magnitude for the Japan data set; the zero-bias value (dashed line) is shown for reference. (c and d) the same as (a) and (b) but for the Italian data set. (e and f) the same as (a) and (b) but for TG data set.

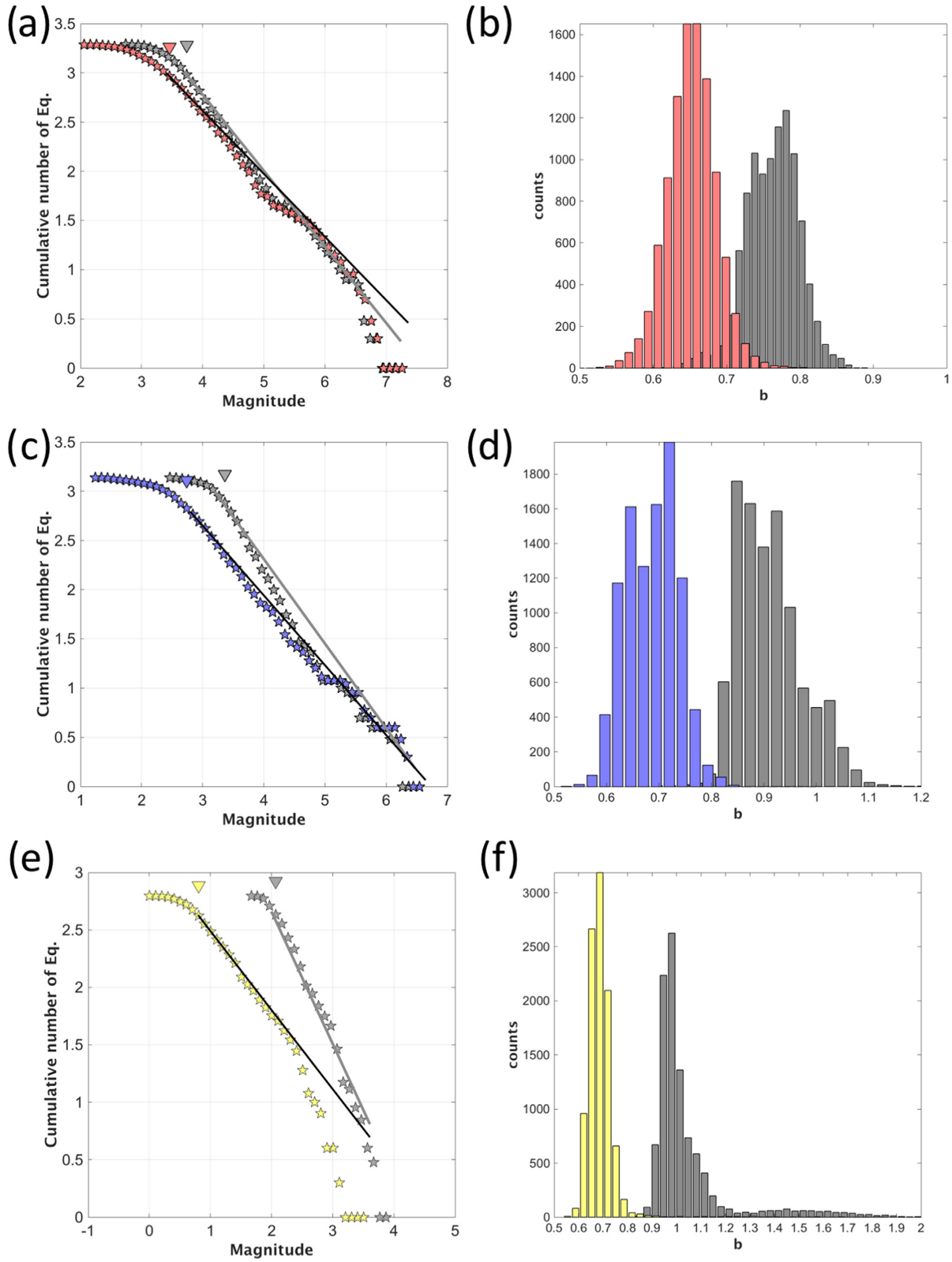

Figure 5. (a) Logarithm of CFM distributions for M_w (grey stars) and M_E (red stars), Gutenberg-Richter law (M_w, grey; M_E, black) and completeness magnitude, M_c (M_w, grey inverse triangle; M_E, red inverse triangle) defined by eq. (5) (by using the maximum-likelihood technique). (b) *b*-value distributions (M_w, grey; M_E, red) derived by bootstrap analysis. (c) as (a), but for the Italian data set (M_E, blue). (d) as (b), but for the Italian data set. (e) as (a), but for TG data set (M_E, yellow). (f) as (b), but for TG data set.

Table 2. Regression parameters of eq. (6) for different data sets and magnitude.

	a	b	σ_b	M_c	σ_{Mc}
M_w – Japan	5.8	0.76	0.02	3.7	0.1
M_e – Japan	5.2	0.65	0.02	3.4	0.1
M_w – Italy	5.9	0.90	0.03	3.3	0.2
M_e – Italy	4.7	0.69	0.02	2.7	0.2
M_w – TG	5.0	1.15	0.03	2.1	0.3
M_e – TG	3.2	0.68	0.03	0.8	0.2

M_w and M_E have a similar trend (Fig. 2a). Bormann & Di Giacomo (2011a) reported that teleseismic Θ estimates collected at global scale tend towards a value of around –4.9, and thus M_E tends on average to be slightly lower than M_w, which agrees well with our findings (Figs 2 and 3a). With respect to the seismicity of moderate-to-large magnitude, we therefore provide evidence confirming that Kanamori's condition is on average fulfilled. Of course, even within this range of moderate-to-large magnitudes, the rupture process of single events can occur under dynamic conditions which deviate from the global average, leading to M_E being larger or smaller than M_w. According to the scheme proposed by Choy (2012), in the first case, $M_E > M_w$ is associated to events characterized by larger shaking potential than the one expected from M_w alone (i.e. earthquakes with particularly high stress drop). In contrast, when the $(M_E - M_w)$ difference is well below <–0.5, the event radiates an abnormally low amount of energy relative to seismic moment (i.e. a category of such events includes the so-called 'slow' earthquakes, typically characterized by low stress drop and generating large tsunamis when they occur at shallow depth in marine subduction zones, Newman & Okal 1998).

In contrast, focusing on the seismicity characterized by smaller magnitudes (approximately $M_w < 5$), our results show that for all three data sets the E_r-to-M_0 scaling progressively diverges from the Kanamori's condition with the decrease in magnitude (Fig. 2). We observe that the radiation of a smaller amount of seismic energy relative to seismic moment is particularly important in the case of TG. Picozzi *et al.* (2017a) showed that the TG seismicity (i.e. mostly induced by the exploitation of the largest geothermal field in the world) is characterized by low stress drop $\Delta\sigma$, and high frequency spectral fall-off parameter (γ) larger than 2 (i.e. whereas 2 is the value of the Brune 1970, source model). Low $\Delta\sigma$ values in the case of induced seismicity in geothermal areas are possibly related to the concomitant effects of different conditions, such as for instance a shallower depth and the injection of fluids that contribute to the effective stress decrease (Goertz-Allmann & Wiemer 2013); furthermore, the high temperatures in geothermal fields can affect the crustal mechanical behaviour, in particular, to reduce the frictional strength. According to Madariaga's dynamic model (1976), the small amount of E_r related to a high γ suggests that most of the TG seismicity is characterized by smooth rupture propagation and, in accordance with Frankel (1991), that the faults strength is not scale-invariant. Accordingly, Picozzi *et al.* (2017a) found that the TG seismicity is characterized by a seismic radiation efficiency η_{SW} indicating positive overshoot (i.e. $\eta_{SW} < 0.3$) and that it deviates from self-similarity. All these considerations, combined with our findings (i.e. the deviation from Kanamori's conditions), suggest that in the case of TG, M_E should be preferred to M_w to appropriately capture the event-to-event variability of the peak ground velocity. Note that, on the contrary, for events with $M_w > 5$ and $\Theta = \Theta_K$, M_w and M_E have similar performance in terms of between-event residuals (δBe; Figs 4a and b). Assessing the potential of magnitude scales in capturing the event-to-event shaking potential capability is an issue that has received special attention during recent years. For instance, Picozzi *et al.* (2018) have recently introduced a rapid response magnitude, which consists of a mix of M_w and M_E combined as a function of the event-specific Θ, with the aim of developing a procedure for the real-time assessment of the earthquake shaking potential.

As discussed by several authors (e.g. Walling 2009; Al Atik *et al.* 2010), reducing the standard deviation (i.e. the sigma) of GMPEs is a fundamental step in reducing the uncertainty in seismic hazard studies. From this perspective, we show that M_E deserves certainly further consideration, especially for carrying out seismic hazard studies in areas where $\Delta\sigma$ values with a strong seismic moment dependency are found (i.e. as observed at TG). Obviously, these considerations can be extrapolated to any other area where the seismicity (indifferently whether this latter is of tectonic or non-tectonic origin) presents characteristics like those observed at TG geothermal field (i.e. $\Theta \neq \Theta_K$, strongly non-self-similar). The seismicity with magnitude lower than M_w 5 that we have observed for the Italian and Japanese data sets shows a smaller deviation from Kanamori's condition with respect to the one of TG, but supports similar conclusions (i.e. as soon as Θ becomes smaller than Θ_K, which corresponds to low $\Delta\sigma$, M_w has a worst performance in predicting the PGV scaling than M_E). Future studies will be directed to verify whether similar conditions hold, as we think, for areas with microseismic activity, where the crust is highly fractured and partially or completely saturated with fluids (e.g. the crust of the Apennine chain in Southern Italy where a M 6.9 earthquake occurred in 1980, Zollo *et al.* 2014). However, we must bear in mind that obtaining robust estimates of seismic source parameters, in particular of the corner frequency and in turn of E_r, for small magnitude earthquakes is still a topic of research and discussion within the seismological community. Deichmann (2018) recently presented a clear exposition of the theoretical background for M_E, M_L and M_w, lighting up how different magnitude scales look at the earthquake source and bringing under the light several common misinterpretations concerning the small magnitude events. Within the framework of the discussion on magnitude scales, we show that for events characterized by low $\Delta\sigma$ values (i.e. for the Italian and especially The Geysers data sets), M_E and M_w perform differently when used to assess the ground motion (i.e. the PGV), with this latter representing an independent information with respect to the magnitude. Our results suggest undertaking a serious thought on the implications of relying on a magnitude metric obtained under conditions far from those on which it has been defined to perform seismic hazard studies. Indeed, while selecting M_w or M_E would have a small impact for hazard studies concerning with earthquakes having $M_w > 5$, this decision might become a crucial one in the case of induced seismicity, if for this latter holds $\Theta \neq \Theta_K$. As also highlighted by Dost *et al.* (2018), the analysis of small magnitude events in the case of induced seismicity is very important because both it represents an imposed risk on society and it can occur in areas where buildings are designed without a proper resistance against seismic shaking.

Similarly to Uchide & Imanishi (2018), who studied the implications of different b values from M_w and the Japan Meteorological Agency magnitude scale (M_j), we investigated if the cumulative frequency–magnitude (CFM) distributions from M_w and M_E present similar features and if they account for the varying dynamic properties of ruptures. Interestingly, for the Japan data set, which is the one presenting dynamic properties closer to Kanamori's condition

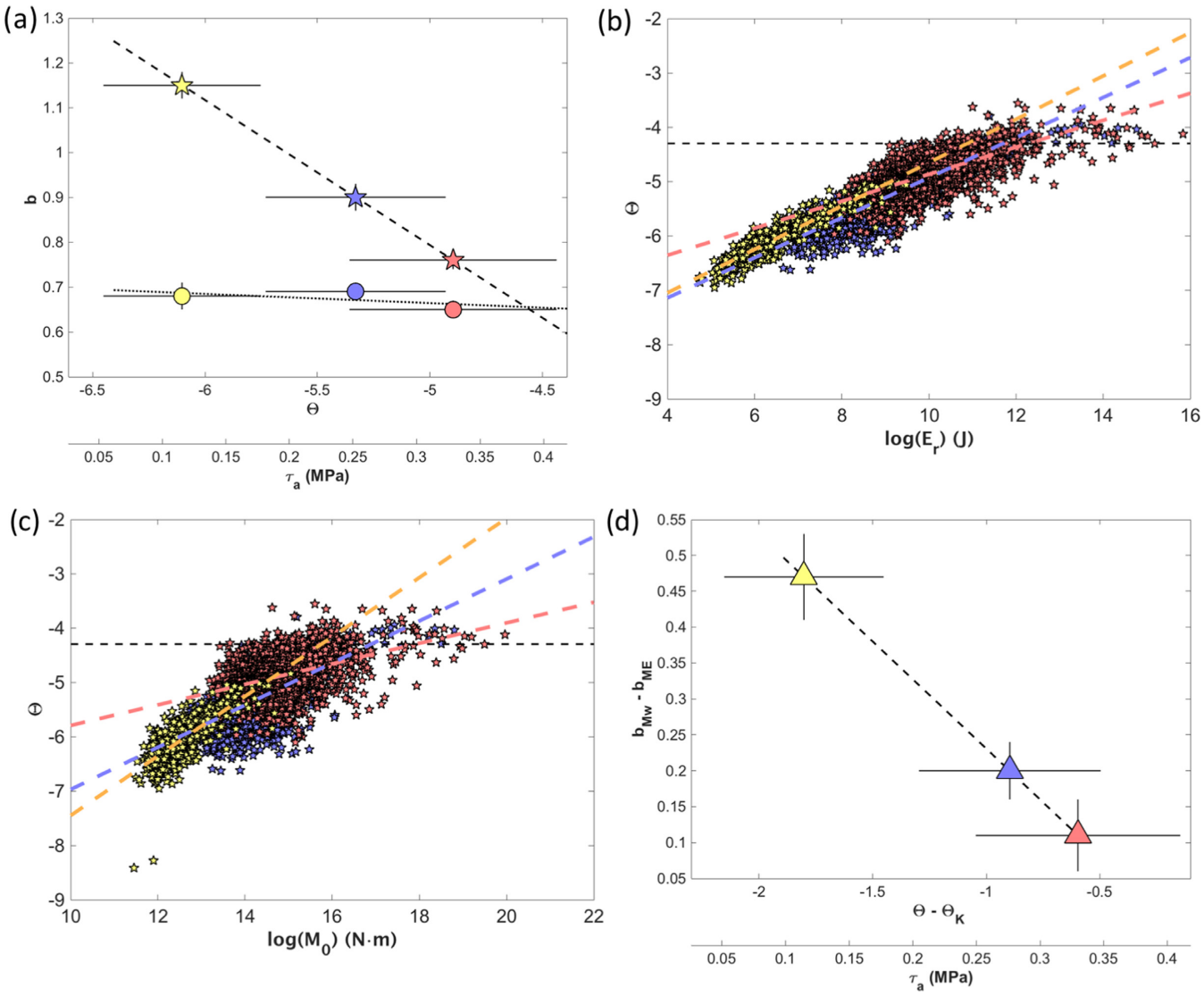

Figure 6. (a) *b*-value for M_w (stars) and M_E (dots) for different data set (Japan, red; Italy, blue; TG, yellow) versus the median Θ and apparent stress, τ_a. Values are plotted together with ± one standard deviation (black line) for both *b* and Θ. The best-fit model for both *b*-values is also represented (black dashed line). (b) Θ versus log(E_r) for different data sets and best-fitting models (stars and dashed lines coloured accordingly to Fig. 1), $Θ_K$ reference value (black dashed line). (c) The same as (b), but Θ versus log(M_0) and best-fitting models. (d) difference ($b_{Mw} - b_{ME}$) versus difference ($Θ - Θ_K$) difference for the four data sets (i.e. the median Θ of each data set is considered), values are plotted together with ± one standard deviation (black line) for both *b* (i.e. in this case the sum of the b_{Mw} and b_{ME} standard deviation) and Θ.

than the others, the two CFM distributions look very similar, whilst for the TG data set (i.e. for which holds $Θ \neq Θ_K$) they differ considerably. Studies on the link between the *b*-value and stress (i.e. especially the deviatoric stress σ_D) have been carried out by different authors across a wide range of scales and conditions (e.g. Amitrano 2003, in laboratory; Schorlemmer *et al.* 2005, and Scholz 2015, at global scale; Bachmann *et al.* 2012, for induced microseismicity generated by an Enhanced Geothermal System, EGS, in Basel, Switzerland). All studies agree on observing an inverse scaling between *b* and σ_D, and we have obtained results which apparently go in the same direction. As shown in (Fig. 6), the difference between the *b*-values for M_w and M_E shows an inverse linear scaling with the difference between Θ and $Θ_K$. These latter observations are also related to the dynamic conditions characterizing the seismicity of each area; for instance, *b*-values for M_w and M_E are different for TG data where the seismicity is non-self-similar (Picozzi *et al.* 2017a), while are similar for the Japanese data where the seismicity is close to self-similar scaling (Oth *et al.* 2010). We found that for all the investigated areas *b* for M_E is nearly constant (i.e. b_{Me} ∼0.7), while the *b*-value from M_w (b_{Mw}) grows with the Θ decrease (i.e. which corresponds to a decrease in the apparent stress). With respect to this last aspect, we think that dealing with two complementary *b* values, one related to seismic moment and the other to radiated seismic energy, would have important implications for seismic hazard studies in areas with induced seismicity presenting $\Delta\sigma$ values with a strong seismic moment dependency.

7 CONCLUSION

In this study, we analysed the source parameters of about 4000 earthquakes recorded at regional/local scale and about 700 from a global data set, covering an overall magnitude range from M_w 1.5

to 9.0. The aim of this work was to investigate the complementary behaviour of M_w and M_E considering data sets covering different geographical areas and extensions, and composed by either natural or induced earthquakes. Despite our study focused on only few regions, and thus caution is recommended on generalizing our conclusion before the analysis of data acquired in many more regions is carried out, we believe that our results can stimulate useful discussions within the seismological community.

The results shown in this work can be summarized consider two different aspects. The first one is related to the results from previous studies and consists in highlighting the trend in the E_r-to-M_0 and M_E-to-M_w scaling as function of $\Delta\sigma$ (Figs 2 and 3). In this sense, our results show that a 1:1 scaling between M_E and M_w only holds when $\Delta\sigma$ is larger than approximately 1 MPa. Whenever $\Delta\sigma$ is smaller, the scaling between M_E and M_w does change. Indeed, M_w and M_E have a common root and, if the stress drop is constant, they are equivalent. The average stress drop then only results in an offset (i.e. one source parameter is enough to describe the source spectrum; Aki 1968). However, if the stress drop is scale-dependent, M_w and M_E are not equivalent but complementary (one cannot play the role of the other), and we have shown that this has implications both for the event-to-event variability of the peak ground velocity and for the characteristics of the cumulative frequency–magnitude distributions.

The other aspect of the results of this work regards the implications of using different magnitude scales for ground motion assessment related analyses (i.e. due to their different sensitivity to different dynamic rupture conditions). With respect to this issue, the main results and considerations coming from our work can be summarized as follows:

(1) M_E does a better job in capturing the high frequency ground shaking variability than M_w in the case of variable stress drop. This issue would be immediately clear if we would calibrate GMPE using directly M_0 (instead of M_w), which would immediately show as the predictor variable for the source is not the suitable one to capture the high frequency variability (which does not influence the seismic moment), whilst the radiated energy is better suited for this task. Somehow using magnitude scales instead of original physical parameters (i.e. M_0 and E_r) masked the implications of assuming M_w as reference magnitude scale for GMPE. We have shown that, for events deviating from the $\Theta = \Theta_K$ condition (i.e. those with low magnitude and low $\Delta\sigma$), if M_w is replaced with M_E the standard deviation of δBe is significantly reduced. This means that M_E allows accounting for variations in those rupture processes introducing systematic event-dependent deviations from the mean regional PGV scaling, and therefore, for seismic hazard studies in areas where anomalously low $\Delta\sigma$ values are found, such as regions where induced seismicity occurs, M_E might be a valid alternative to M_w for deriving GMPE. If low frequencies, earthquake-generated tsunami studies or tectonic aspects are of interest, M_w is still the best choice.

(2) From a more seismic hazard-oriented perspective (even if we are not carrying out any hazard assessment in this work), considering the cumulative frequency–magnitude distribution for M_E and M_w for different data sets, we have shown that the b values, one related to seismic moment (b_{Mw}) and the other to radiated seismic energy (b_{ME}), are significantly different. In particular, b_{ME} is nearly constant for all data sets, while b_{Mw} shows an inverse linear scaling with Θ and the apparent stress. It is worth noting that both b_{ME} and b_{Mw} are 'correct', simply, their meaning is different. Indeed, in one case the distribution is describing the cumulative number of events having seismic moment greater than a given value, the other the cumulative distribution for the energy. From this perspective, the use of one rather than the other should depend on the task of interest, but we think that their complementary nature should be considered for seismic hazard studies, in particular when dealing with low stress-drop induced seismicity.

ACKNOWLEDGEMENTS

We would like to thank the Editor E. Hauksson and two anonymous reviewers for their comments and suggestions that allowed us to significantly improve the manuscript content and form. All data used in this work are already published and we refer to previous studies for their availability (i.e. Global, Di Giacomo *et al.* 2011a; Japan, Oth 2013; Italy, Bindi *et al.* 2017; The Geysers, Picozzi *et al.* 2017). For readers' convenience, we included as supplemental material files with seismic moment and radiated energy for the regional data sets. This study has been partially funded by the H2020-INFRAIA project SERA (Seismology and Earthquake Engineering Research Infrastructure Alliance for Europe).

REFERENCES

Aki, K., 1965. Maximum likelihood estimation of b in the formula log N = a-bM and its confidence limits, *Bull. seism. Soc. Am.,* **43,** 237–239.

Aki, K., 1967. Scaling law of seismic spectrum, *J. geophys. Res.,* **72**(4), 1217–1231.

Aki, K., 1968. Seismic displacements near a fault, *J. geophys. Res.,* **73**(16), 5359–5376.

Al Atik, L., Abrahamson, A., Bommer, J.J., Scherbaum, F., Cotton, F. & Kuehn, N., 2010. The variability of ground-motion prediction models and its components. *Seismol. Res. Lett.,* **81**(5), 794–801.

Amitrano, D., 2003. Brittle-ductile transition and associated seismicity: experimental and numerical studies and relationship with the b value, *J. geophys. Res.,* **108**(B1), 2044.

Anderson, J.G., 1997. Seismic energy and stress-drop parameters for a composite source model, *Bull. seism. Soc. Am.,* **87,** 85–96.

Anderson, J.G. & Lei, Y., 1994. Nonparametric description of peak acceleration as a function of magnitude, distance, and site in Guerrero, Mexico, *Bull. seism. Soc. Am.,* **84,** 1004–1017.

Atkinson, G.M., 1995. Optimal choice of magnitude scales for seismic hazard analysis, *Seismol. Res. Lett.,* **66**(1), 51–55.

Bachmann, C., Wiemer, S., Goertz-Allmann, B.P. & Woessner, J., 2012. Influence of pore pressure on the size distribution of induced earthquakes, *Geophys. Res. Lett.,* **39,** L09302.

Baltay, A., Hanks, T. & Beroza, G., 2013. Stable stress-drop measurements and their variability: implications for ground-motion predictions, *Bull. seism. Soc. Am.,* **103,** 211–222.

Baltay, A.S., Hanks, T.C. & Abrahamson, N.A., 2017. Uncertainty, variability, and earthquake physics in ground-motion prediction equations. *Bull. seism. Soc. Am.* **107,** 1754–1772.

Bindi, D., Luzi, L., Pacor, F., Franceschina, G. & Castro, R.R., 2006. Ground-motion predictions from empirical attenuation relationships versus recorded data: the case of the 1997–1998 Umbria-Marche, central Italy, strong-motion data set, *Bull. seism. Soc. Am.,* **96,** 984–1002.

Bindi, D., Spallarossa, D. & Pacor, F., 2017. Between-event and between-station variability observed in the Fourier and response spectra domains: comparison with seismological models, *Geophys. J. Int.,* **210,** 1092–1104.

Bindi, D., Spallarossa, D., Picozzi, M., Scafidi, D. & Cotton, F., 2018. Impact of magnitude selection on aleatory variability associated with Ground Motion Prediction Equations: Part I – local, energy and moment magnitude calibration for Central Italy, *Bull. seism. Soc. Am.*

Boettcher, M.S., Kane, D.L., McGarr, A., Johnston, M.J.S. & Reches, Z., 2015. Moment tensors and other source parameters of mining-induced earthquakes in TauTona Mine, South Africa, *Bull. seism. Soc. Am.,* **105**(3), 1576–1593.

Bommer, J.J. & Alarcón, J.E., 2006. The prediction and use of peak ground velocity. *J. Earthq. Eng.,* **10**(1), 1–31.

Bormann, P., 2015. Are new data suggesting a revision of the current Mw and Me scaling formulas? *J. Seismol.,* **19,** 989–1002.

Bormann, P. & Di Giacomo, D., 2011a. The moment magnitude Mw and the energy magnitude Me: common roots and differences. *J Seismol,* **15,** 411–427.

Bormann, P. & Di Giacomo, D., 2011b. Earthquakes, energy, in *Encyclopedia of Solid Earth Geophysics,*pp. 233–237, Springer Nature.

Bradley, B.A., 2012. Empirical correlation between cumulative absolute velocity and amplitude-based ground motion intensity measures, *Earthquake Spectra,* doi: 10.1193/1.3675580.

Brune, J.N., 1970. Tectonic stress and the spectra of seismic shear waves from earthquakes. *J. geophys. Res.,* **75,** 4997–5009.

Burroughs, S.M. & Tebbens, S.F., 2002. The Upper-Truncated power law applied to Earthquake cumulative Frequency–Magnitude distributions: Evidence for a Time-Independent scaling parameter, *Bull. seism. Soc. Am.,* **92**(8), 2983–2993.

Castro, R.R., Anderson, J.G. & Singh, S.K., 1990. Site response, attenuation and source spectra of S waves along the Guerrero, Mexico, subduction zone, *Bull. seism. Soc. Am.,* **80**(6), 1481–1503.

Choy, G.L., 2012. Stress conditions inferable from modern magnitudes: development of a model of fault maturity. IS3.5in *New Manual of Seismological Observatory Practice (NMSOP-2), IASPEI, GFZ German Research Centre for Geosciences, Potsdam*; ed. Bormann, P.http://nmsop.gfz-potsdam.de, doi:10.2312/GFZ.NMSOP-2.

Choy, G.L. & Boatwright, J., 1995. Global patterns of radiated seismic energy and apparent stress, *J. geophys. Res.,* **100**(18), 205–226.

Convertito, V., Maercklin, N., Sharma, N. & Zollo, A., 2012. From induced seismicity to direct time-dependent seismic hazard, *Bull. seism. Soc. Am.,* **102,** 2563–2573.

Courboulex, F., Vallée, M., Causse, M. & Chounet, A., 2016. Stress-drop variability of shallow earthquakes extracted from a global database of source time functions, *Seismol. Res. Lett.,* **87**(4), 912–918.

Deichmann, N., 2018. The relation between M_E, M_L and M_w in theory and numerical simulations for small to moderate earthquakes, *J. Seismol.,* **22,** 1645.

Di Giacomo, D., Parolai, S., Bormann, P., Grosser, H., Saul, J., Wang, R. & Zschau, J., 2010. Suitability of rapid energy magnitude estimations for emergency response purposes, *Geophys. J. Int.,* **180,** 361–374.

Di Giacomo, D. & Bormann, P., 2011. The moment magnitude Mw and the energy magnitude Me: common roots and differences, *J. Seismol.,* **15,** 411–427.

Dost, B., Edwards, B. & Bommer, J.J., 2018. The relationship between M and M_L: a review and application to induced seismicity in the groningen gas field, The Netherlands, *Seismol. Res. Lett.,* **28**(89), 1062–1074.

Douglas, J. & Edwards, B., 2016. Recent and future developments in earthquake ground motion estimation, *Earth Sci. Rev.,* **160,** 203–219.

Dziewonski, A.M., Chou, T.A. & Woodhouse, J.H., 1981. Determination of earthquake source parameters from waveform data for studies of global and regional seismicity, *J. Geophys Res.,* **86,** 2825–2852.

Ekström, G., Nettles, M. & Dziewonski, A.M., 2012. The global CMT project 2004–2010: centroid-moment tensors for 13,017 earthquakes, *Phys. Earth planet. Inter.,* **200–201,** 1–9.

Efron, B., 1979. Bootstrap methods: another look at the jackknife, *Ann. Stat.,* **7**(1), 1–26.

Goertz-Allmann, B.P. & Wiemer, S., 2013. Geomechanical modeling of induced seismicity source parameters and implications for seismic hazard assessment, *Geophysics,* **78**(1), KS25–KS39.

Gutenberg, B., 1945a. Amplitudes of P PP, and S and magnitude of shallow earthquake. *Bull. seism. Soc. Am.,* **35,** 57–69.

Gutenberg, B., 1945b. Magnitude determination of deep-focus earthquakes, *Bull. seism. Soc. Am.,* **35,** 117–130.

Gutenberg, B. & Richter, C.F., 1942. Earthquake magnitude, intensity, energy, and acceleration, *Bull. seism. Soc. Am.,* **32,** 163–191.

Gutenberg, B. & Richter, C.F., 1956. Magnitude and energy of earthquakes, *Ann. Geofisica,* **9,** 1–15.

Hanks, T.C. & Kanamori, H., 1979. A moment magnitude scale, *J. geophys. Res.,* **84,** 2348–2350.

Ide, S. & Beroza, G.C., 2001. Does apparent stress vary with earthquake size? *Geophys. Res. Lett.,* **28,** 3349–3352.

Izutani, Y. & Kanamori, H., 2001. Scale-dependence of seismic energy-to-moment ratio for strike-slip earthquakes in Japan, *Geophys. Res. Lett.,* **28,** 4007–4010.

Kanamori, H., 1977. The energy release in great earthquakes, *J. geophys. Res.,* **82,** 2981–2876.

Kanamori, H., 1983. Magnitude scale and quantification of earthquakes, *Tectonophysics,* **93,** 185–199.

Kanamori, H. & Anderson, D.L., 1975. Theoretical basis of some empirical relations in seismology, *Bull. seism. Soc. Am.,* **65,** 1073–1095.

Kwiatek, G., Plenkers, K., Nakatani, M., Yabe, Y. & Dresen, G., JAGUAR-Group, 2010. Frequency-magnitude char- acteristics down to magnitude −4.4 for induced seismicity recorded at Mponeng Gold Mine, South Africa, *Bull. seism. Soc. Am.,* **100**(3), 1165–1173.

Kwiatek, G. & Ben-Zion, Y., 2016. Theoretical limits on detection and analysis of small earthquakes, *J. geophys. Res.,* **121,** 5898–5916.

Frankel, A., 1991. Mechanisms of seismic attenuation in the crust: scattering and anelasticity in New York State, South Africa, and southern California, *J. geophys. Res.,* **96**(B4), 6269–6289.

Madariaga, R., 1976. Dynamics of an expanding circular fault, *Bull. seism. Soc. Am.,* **66,** 639–666.

Main, I., 2000. Apparent breaks in scaling in the earthquake cumulative frequency-magnitude distribution: fact or artefact? *Bull. seism. Soc. Am.,* **90**(1), 86–97.

Newman, A.V. & Okal, E.A., 1998. Teleseismic estimates of radiated seismic energy: the Er/Mo discriminant for tsunami earthquakes, *J. geophys. Res.,* **103,** 26,885–26,898.

Okada, Y., Kasahara, K., Hori, S., Obara, K., Sekiguchi, S., Fujiwara, H. & Yamamoto, A., 2004. Recent progress of seismic observation networks in Japan-Hi-net, F-net, K-NET and KiK-net, *Earth Planets Space,* **56,** xv–xxviii.

Oth, A., 2013. On the characteristics of earthquake stress release variations in Japan, *Earth planet. Sci. Lett.,* **377–378,** 132–141.

Oth, A., Bindi, D., Parolai, S. & Di Giacomo, D., 2010. Earthquake scaling characteristics and the scale-(in)dependence of seismic energy-to-moment ratio: Insights from KiK-net data in Japan, *Geophys. Res. Lett.,* **37,** L19304, doi:10.1029/2010GL044572.

Oth, A., Bindi, D., Parolai, S. & Giacomo, D.D., 2011. Spectral analysis of K-NET and KIK-net data in Japan, Part II: on attenuation characteristics, source spectra, and site response of borehole and surface stations, *Bull. seism. Soc. Am.,* **101**(2), 667–687.

Oth, A., Miyake, H. & Bindi, D., 2017. On the relation of earthquake stress drop and ground motion variability, *J. geophys. Res.: Solid Earth,* **122,** 5474–5492.

Orowan, E., 1960. Mechanisms of seimic faulting in rock deformation: a symposium, *Geol. Soc. Am. Mem.,* **79,** 323–345.

Oye, V., Bungum, H. & Roth, M., 2005. Source parameters and scaling relations for mining-related seismicity within the Pyha ¨salmi Ore Mine, Finland, *Bull. seism. Soc. Am.,* **95**(3), 1011–1026.

Pace, B., Peruzza, L., Lavecchia, G. & Boncio, P., 2006. Layered seismogenic source model and probabilistic seismic-hazard analyses in central Italy, *Bull. seism. Soc. Am.,* **96,** 107–132.

Pacheco, J.F., Scholz, C.H. & Sykes, L.R., 1992. Changes in frequency- size relationship from small to large earthquakes, *Nature,* **355,** 71–73.

Picozzi, M., Oth, A., Parolai, S., Bindi, D., De Landro, G. & Amoroso, O., 2017a. Accurate estimation of seismic source parameters of induced seismicity by a combined approach of generalized inversion and genetic algorithm: application to The Geysers geothermal area, California, *J. geophys. Res.: Solid Earth,* 122, doi:10.1002/2016JB013690.

Picozzi, M., Bindi, D., Brondi, P., Di Giacomo, D., Parolai, S. & Zollo, A., 2017b. Rapid determination of P wave- based energy magnitude: insights on source parameter scaling of the 2016 Central Italy earthquake sequence, *Geophys. Res. Lett.,* **44,** 4036–4045.

Picozzi, M., Bindi, D., Spallarossa, D., Di Giacomo, D. & Zollo, A., 2018. A rapid response magnitude scale for timely assessment of the high frequency seismic radiation, *Scientific Reports – Nature,* **8,** 8562.

Purcaru, G. & Berckhemer, H., 1978. A magnitude scale for very large earthquakes, *Tectonophysics,* **49,** 189–198.

Richter, C., 1935. An instrumental earthquake magnitude scale, *Bull. seism. Soc. Am.,* **25,** 1–32.

Richter, C.F., 1958. *Elementary Seismology,* pp. viii+768, W. H. Freeman and Company.

Scholz, C.H., 1997. Size distributions for large and small earthquakes, *Bull. seism. Soc. Am.,* **87,** 1074–1077.

Scholz, C.H., 2015. On the stress dependence of the earthquake b value, *Geophys. Res. Lett.,* **42,** 1399–1402.

Schorlemmer, D., Wiemer, S. & Wyss, M., 2005. Variations in earthquake-size distribution across different stress regimes, *Nature,* **437**(7058), 539–542.

Trugman, D.T. & Shearer, P.M., 2018. Strong correlation be tween stress drop and peak ground acceleration for recent Earthquakes in the San Francisco Bay Area, *Bull. seism. Soc. Am.,* **108,** 929–945.

Uchide, T. & Imanishi, K., 2018. Underestimation of microearthquake size by the magnitude scale of the Japan Meteorological Agency: influence on earthquake statistics, *J. geophys. Res.: Solid Earth,* 123, doi:10.1002/2017JB014697.

Utsu, T., 1965. A method for determining the value of b in the formula log*n* = a − bM showing the magnitude–frequency relation for earth- quakes (with English summary), *Geophys. Bull. Hokkaido Univ.,* **13,** 99–103.

Venkataraman, A. & Kanamori, H., 2004. Observational constraints on the fracture energy of subduction zone earthquakes, *J. geophys. Res.,* **109,** B05302, doi:10.1029/2003JB002549.

Venkataraman, A., Rivera, L. & Kanamori, H., 2002. Radiated energy from the 16 October 1999 Hector Mine Earthquake: regional and teleseismic estimates, *Bull. seism. Soc. Am.,* **92,** 1256–1266.

Walling, M.A., 2009. Non-ergodic probabilistic seismic hazard analysis and spatial simulation of variation in ground motion, *PhD diss.*, University of California, Berkeley.

Woessner, J. & Wiemer, S., 2005. Assessing the quality of earthquake catalogs: estimating the magnitude of completeness and its uncertainties, *Bull. seism. Soc. Am.,* **95**(2), 684–698.

Worden, C.B., Wald, D.J., Allen, T.I., Lin, K., Garcia, D. & Cua, G., 2010. A revised ground-motion and intensity interpolation scheme for ShakeMap, *Bull. seism. Soc. Am.,* **100**(6), 3083–3096.

Wiemer, S., 2001. A software package to analyze seismicity: ZMAP, *Seismol. Res. Lett.,* **72,** 373–382.

Zollo, A., Orefice, A. & Convertito, V., 2014. Source parameter scaling and radiation efficiency of microearthquakes along the Irpinia fault zone in southern Apennines, Italy, *J. geophys. Res.: Solid Earth,* **119,** 3256–3275.

SUPPORTING INFORMATION

Supplementary data are available at *GJI* online.

Figure S1. comparison of E_r estimates for the Japanese data set obtained by Oth (2013) integrating the empirical source spectra from the GIT and the extrapolation with a Brune source model outside the frequency vs the integration of the Brune source model obtained using M_0 and f_c from the same study.

Figure S2. E_r-to-M_0 scaling for the Japanese (red) and Italian (blue) data sets.

Please note: Oxford University Press is not responsible for the content or functionality of any supporting materials supplied by the authors. Any queries (other than missing material) should be directed to the corresponding author for the paper.